

# Effect of elastomer functionality on toughened PET

V. Tanrattanakul\*, A. Hiltner† and E. Baer

Department of Macromolecular Science and Center for Applied Polymer Research,  
Case Western Reserve University, Cleveland, OH 44106, USA

and W. G. Perkins and F. L. Massey

Polyester Technical Center, Shell Chemical Company, Akron, OH 44305, USA

and A. Moet

Department of Chemical and Petroleum Engineering, United Arab Emirate University, Al-Ain,  
UAE

(Received 3 October 1996)

Poly(ethylene terephthalate) (PET) was blended with up to 5% of an SEBS elastomer. The elastomer was functionalized with 0 to 4.5 wt% maleic anhydride grafted onto the ethylene-butylene midblock. Graft copolymer formed by reaction of PET hydroxyl end groups with the anhydride *in situ* was thought to act as an emulsifier to decrease interfacial tension and promote adhesion. All the elastomers increased the melt viscosity of PET, however the amount and functionality of the elastomer did not have a large effect on blend rheology. In contrast, particle size was strongly dependent on the elastomer functionality: the higher the functionality, the smaller the particle size and the narrower the particle size distribution. Furthermore, elastomer content had less effect on the particle size as the functionality increased, and the tendency toward increasing particle size with increasing elastomer content diminished. These trends were attributed to an increase in the degree of grafting on the *in situ* graft copolymer. Particles of functionalized SEBS were primarily spherical in injection moulded blends in contrast to the highly elongated particles of unfunctionalized SEBS. In un-notched tensile tests, blending PET with any SEBS elastomer enhanced the stability of the propagating neck. Notched tensile tests differentiated among the blends in terms of their toughness. The least effective elastomer was the unfunctionalized SEBS. The most effective was the SEBS with only 1% anhydride. The decrease in toughness with increasing functionality was attributed to decreasing particle size. © 1997 Elsevier Science Ltd.

(Keywords: poly(ethylene terephthalate) blends; rubber toughening; block copolymers)

## INTRODUCTION

A previous paper described the toughening that can be achieved by blending 1–5% of a functionalized triblock copolymer with poly(ethylene terephthalate) (PET)<sup>1</sup>. The triblock copolymer had styrene end blocks and an ethylene/butylene midblock grafted with 2 wt% maleic anhydride. The observations were consistent with *in situ* formation of a graft copolymer by reaction of PET hydroxyl end groups with the anhydride. It appeared that the graft copolymer acted as an emulsifier to decrease the interfacial tension and reduce the tendency of dispersed particles to coalesce during processing. In the solid state, the graft copolymer promoted adhesion between the phases and facilitated cavitation in a triaxial stress state.

When a functionalized SEBS elastomer is used to toughen PET, it can be anticipated that both particle size and interfacial strength will be affected by the composition and amount of graft copolymer that forms in the

reaction with PET. For the present study, variation in graft copolymer structure was achieved by blending PET with SEBS elastomers that had essentially the same styrene-to-ethylene/butylene ratio and the same molecular weight, but varied in the amount of grafted anhydride from 0 to 4.5 wt%. The rheology, solid state structure and mechanical properties of the PET blends were subsequently examined. Performance in a notched tensile test was used to compare toughness and notch sensitivity of the blends.

## EXPERIMENTAL

The PET provided by the Shell Chemical Company (Akron, OH) was Cleartuf<sup>®</sup> 7207, a bottle grade resin with an intrinsic viscosity of 0.73 dl g<sup>-1</sup>, molecular weights of  $M_n = 24\,000$  and  $M_w = 49\,000$ , and hydroxyl number of 1.4 mol mol<sup>-1</sup>. Four SEBS elastomers with essentially the same composition and molecular weight were also provided by the Shell Chemical Company. The elastomers varied in the amount of grafted maleic anhydride, and are identified as SEBS-0MA (Kraton<sup>®</sup> G1652 with 0% anhydride), SEBS-1MA (Kraton<sup>®</sup>

\* Present address: Department of Chemistry, Prince of Songkla University, Songkla, Thailand

† To whom correspondence should be addressed

FG1921X with 1 wt% grafted anhydride), SEBS-2MA (Kraton<sup>®</sup> FG1901X with 2 wt% grafted anhydride), and SEBS-4.5MA (Kraton<sup>®</sup> B51-4 with 4.5 wt% grafted anhydride). The ratio of styrene to ethylene/butylene was 28/72 by weight, and the glass transition temperature of the EB block was  $-42^{\circ}\text{C}$ . The styrene equivalent molecular weights were approximately 75 000 ( $M_n$ ) and 77 000 ( $M_w$ ) for SEBS-0MA and SEBS-2MA, and 71 000 ( $M_n$ ) and 73 000 ( $M_w$ ) for SEBS-1MA and SEBS-4.5MA.

The components were dried and melt blended in a twin screw extruder as described previously<sup>1</sup>. Blends with 1, 2 and 5% elastomer by weight were processed with a barrel temperature of  $280^{\circ}\text{C}$  and screw speed of 35 rpm. Blends with 2% elastomer were also processed at a lower temperature ( $260^{\circ}\text{C}$ ) with two screw speeds (20 and 35 rpm). Melt viscosities of the extruded blend materials were determined at 260 and  $280^{\circ}\text{C}$  as described previously<sup>1</sup>.

The pellets were injection moulded into a family mould that consisted of a 3.18 mm thick Type I tensile bar (ASTM D638), a 3.18 mm thick Izod impact bar (ASTM D256) and a disc 1.10 mm thick and 50 mm in diameter using conditions described previously<sup>1</sup>. The Izod bars were notched according to ASTM D256 with a  $45^{\circ}$  notch having a 0.25 mm radius and 2.54 mm depth. Pellets from the twin screw extruder and injection moulded tensile bars were freeze-fractured, etched with THF to remove SEBS, and examined in the scanning electron microscope. Particle size distributions were obtained by measuring 300–500 particle diameters<sup>1</sup>.

Tensile and impact testing was carried out on specimens equilibrated under ambient conditions. Unnotched tensile tests were made on Type I tensile bars with a strain rate of  $100\% \text{ min}^{-1}$ . Blends with 5% elastomer were also tested at a strain rate of  $1000\% \text{ min}^{-1}$ . Five specimens were tested for each condition. Tensile tests were also performed on notched Izod bars. The distance between grips was 50 mm and the crosshead speed was  $500 \text{ mm min}^{-1}$ . Tests were made at 25, 0,  $-20$  and  $-40^{\circ}\text{C}$ . Specimens were equilibrated in the Instron machine at the test temperature for 10 min before testing.

Puncture tests were carried out on a DYNATUP 8250 instrument following ASTM D3763. The plunger was dropped a height of 300 mm which produced a velocity of  $1.5 \times 10^5 \text{ mm min}^{-1}$  on impact. The plunger had a hemispherical tup with a 12.7 mm diameter. Five specimens were tested at 25 and  $-29^{\circ}\text{C}$ . The specimens were maintained at temperature overnight before testing. The notched Izod impact strength was measured at ambient temperature using a TMI No. 43-1 impact tester with impact speed of  $2 \times 10^5 \text{ mm min}^{-1}$ . Ten specimens were tested.

## RESULTS AND DISCUSSION

### Blend rheology

The viscosities of the blend components at  $280^{\circ}\text{C}$  are compared in Figure 1a. The decreased viscosity of PET after extrusion under conditions that mimicked the blending process was a result of decreased molecular weight<sup>1</sup>. The viscosity of the unfunctionalized SEBS-0MA was significantly higher than the viscosity of extruded PET. In contrast, the viscosities of the functionalized SEBS elastomers were all lower than that of extruded PET and there were no significant

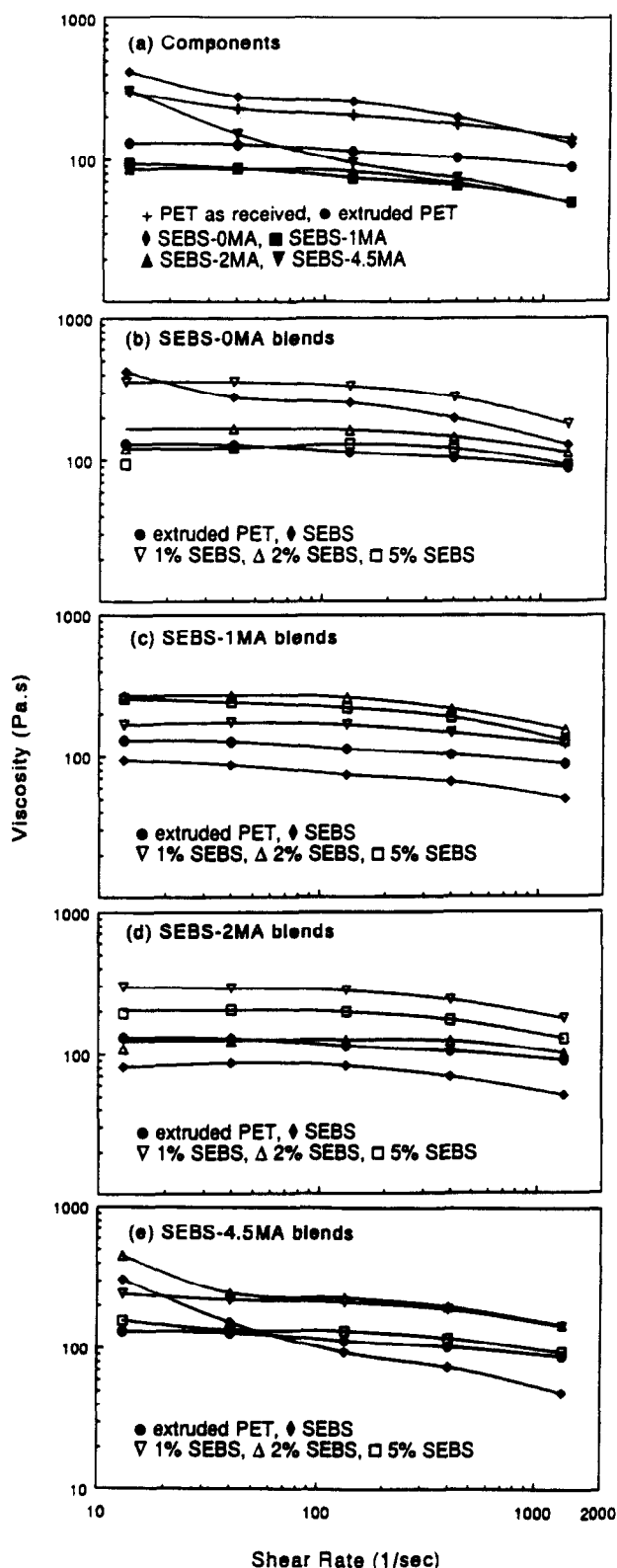


Figure 1 Melt viscosity at  $280^{\circ}\text{C}$ : (a) extruded PET and the four SEBS elastomers; (b) effect of SEBS-0MA; (c) effect of SEBS-1MA; (d) effect of SEBS-2MA; and (e) effect of SEBS-4.5MA. PET and the blends were processed at  $280^{\circ}\text{C}/35 \text{ rpm}$  unless indicated otherwise

differences among the viscosities of the three functionalized elastomers. Compared to PET, the melt viscosity of the elastomers decreased more rapidly with shear rate as reflected in lower values of the power law index ( $n$ ), Table 1. The increase in  $n$  with temperature was consistent with previous results<sup>1</sup>.

**Table 1** Power law index ( $n$ ) of blends and their components

Material	Processing conditions	$n$	
		260°C	280°C
PET	as received	0.74	0.74
	280°C/35 rpm	0.79	0.89
SEBS-0MA	as received	0.56	0.70
SEBS-1MA		0.68	0.83
SEBS-2MA		0.72	0.78
SEBS-4.5MA		0.58	0.72
1% SEBS-0MA	280°C/35 rpm	0.62	0.73
2% SEBS-0MA		0.66	0.84
5% SEBS-0MA		0.67	0.85
1% SEBS-1MA	280°C/35 rpm	0.75	0.86
2% SEBS-1MA		0.72	0.77
5% SEBS-1MA		0.67	0.77
1% SEBS-2MA	280°C/35 rpm	0.69	0.80
2% SEBS-2MA		0.80	0.90
5% SEBS-2MA		0.69	0.81
1% SEBS-4.5MA	280°C/35 rpm	0.75	0.83
2% SEBS-4.5MA		0.73	0.81
5% SEBS-4.5MA		0.78	0.85

Viscosities of the blends at 280°C are compared with the viscosity of extruded PET in *Figures 1b–e*. All the elastomers caused the viscosity of PET to increase. This is consistent with the general observation that the viscosity of a thermoplastic increases when it is modified with an elastomer<sup>2</sup>. Chemical interaction between the phases in a reactive blend system may result in even higher viscosities<sup>3</sup>. If the elastomer has a lower viscosity than the thermoplastic, these trends necessarily produce a maximum in the viscosity–composition curve. Blends of functionalized SEBS with PET exemplified this behaviour. Even blends with unfunctionalized SEBS-0MA, which had a higher viscosity than PET, appeared to exhibit a maximum in the viscosity–composition curve at 1% elastomer; at higher elastomer content, the viscosity decreased to values intermediate between PET and SEBS-0MA. The power law index of the blends always increased with temperature, but it did not show any consistent trends with either elastomer functionality or elastomer content (*Table 1*). Furthermore, neither the viscosity nor the power law index appeared to be affected significantly by processing conditions.

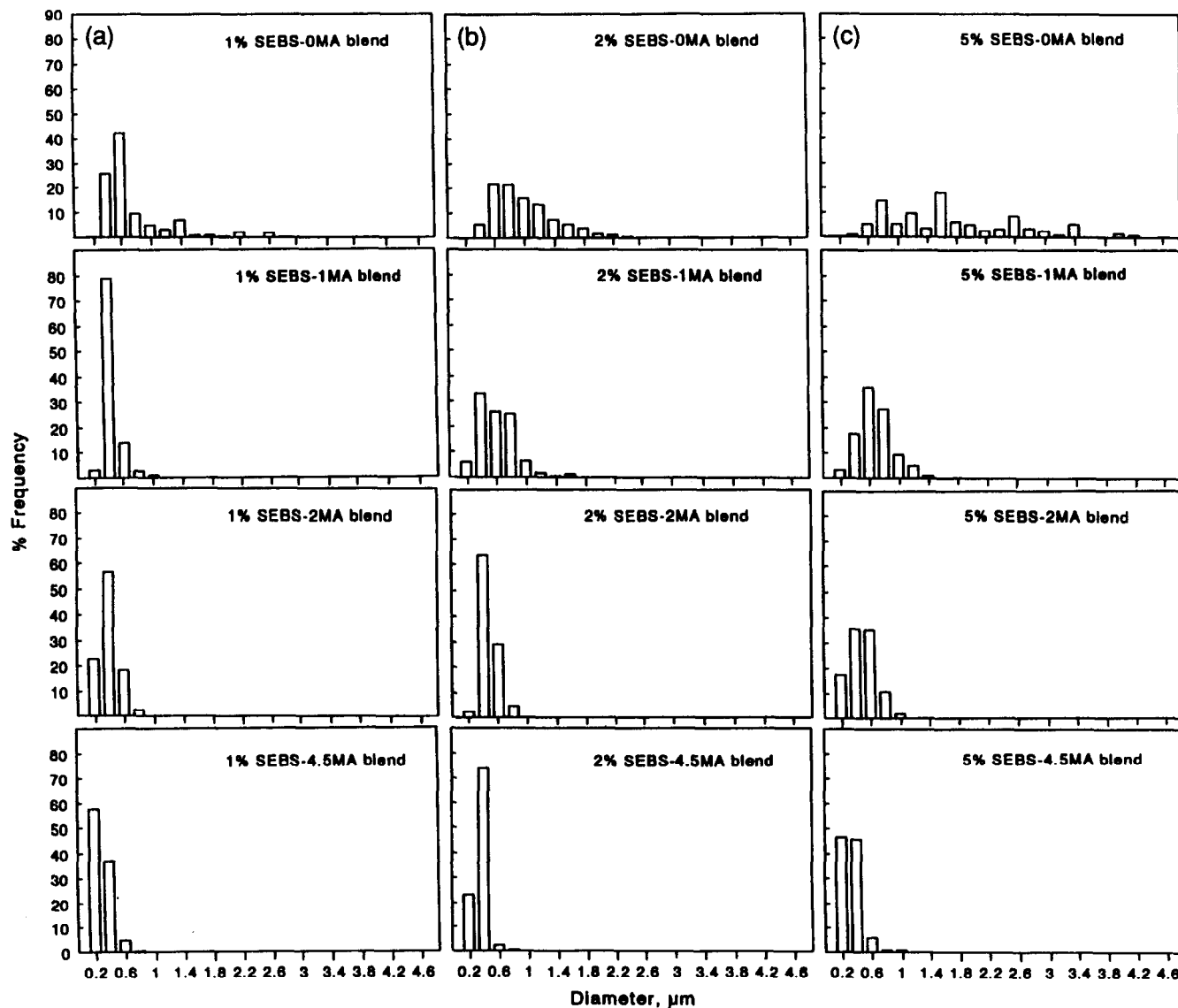


**Figure 2** Particle size distribution in blends processed at 280°C/35 rpm: (a) blends with 1% SEBS elastomer; (b) blends with 2% SEBS elastomer; and (c) blends with 5% SEBS elastomer

Table 2 Average particle diameters

% SEBS	Processing conditions	SEBS-0MA	SEBS-1MA	SEBS-2MA	SEBS-4.5MA
1	280°C/35 rpm	0.69 ± 0.47	0.35 ± 0.13	0.31 ± 0.12	0.21 ± 0.09
2		0.91 ± 0.43	0.50 ± 0.20	0.39 ± 0.12	0.24 ± 0.08
5		1.60 ± 0.97	0.60 ± 0.23	0.39 ± 0.17	0.24 ± 0.12
2	280°C/35 rpm	0.91 ± 0.43	0.50 ± 0.20	0.39 ± 0.12	0.24 ± 0.08
	260°C/35 rpm	1.05 ± 0.49	0.52 ± 0.24	0.40 ± 0.12	0.24 ± 0.12
	260°C/20 rpm	0.98 ± 0.53	0.50 ± 0.20	0.33 ± 0.16	0.28 ± 0.12

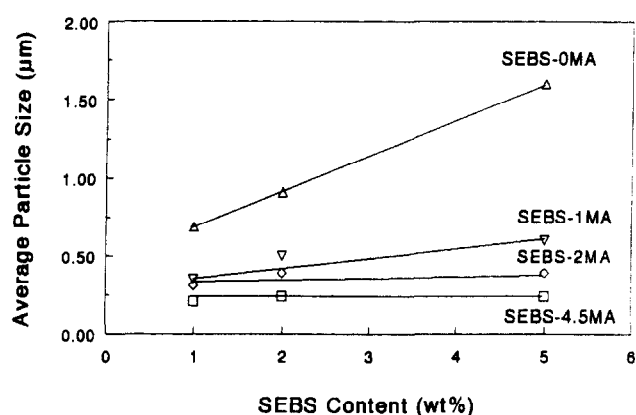


Figure 3 Average particle size as a function of SEBS elastomer content

#### Blend morphology

Unetched and etched freeze-fracture surfaces of the pellets showed the elastomer to be dispersed as spherical particles in all the blends with functionalized SEBS, and as spherical particles mixed with cylindrical shapes in the blends with unfunctionalized SEBS-0MA. Several trends were apparent in the dependence of particle size and size distribution on the degree of elastomer functionality (Figure 2). For a given elastomer content, the average particle size decreased and the size distribution narrowed with increasing functionality (Table 2). This trend was evident for all three elastomer levels examined. Elastomer content also affected particle size and size distribution. In blends of SEBS-0MA, the average particle size more than doubled (0.7–1.6 µm) and the particle size distribution broadened considerably as the elastomer content increased from 1 to 5%. Elastomer content had less effect on particle size and size distribution as the functionality of the elastomer increased. Although the trend toward increasing particle size and broader size distribution with increasing elastomer content was clear in blends with SEBS-1MA, elastomer content had almost no effect on the average particle size or the narrow particle size distribution in blends with SEBS-2MA and SEBS-4.5MA (Figure 3). Particle sizes for blends prepared under different processing conditions, included in Table 2, showed no significant effect of extrusion temperature or shear rate.

Injection mouldings of the blends exhibited a skin-core morphology. This was characterized by examining the edge and the centre of tensile specimens that were freeze-fractured parallel and perpendicular to the injection direction and then etched to remove the SEBS phase. The elastomer domains in the blend with 5%

SEBS-0MA were elongated in the injection direction through the entire thickness (Figure 4). In the skin region, which extended inward about 300 µm, the domains were about 0.5 µm thick. Their elongated shape when viewed perpendicular to the injection direction indicated that the domains in the skin region were platelet-shaped with a large range in the length and width. The aspect ratio in the length varied from 6 to 33:1, and in the width varied from 2 to 20:1. In the centre, the elongated domains were thicker, about 1 µm in diameter, and longer with aspect ratios of 2–80:1. The circular cross-section in the perpendicular direction indicated that they were cylindrical.

The skin of injection mouldings with functionalized SEBS was thinner, about 100 µm. The particles in the skin were platelet-shaped with smaller aspect ratios than in the skin of the SEBS-0MA blends. Particles in the skin of the 5% SEBS-2MA blend, illustrated in Figure 5, were about 0.5 µm thick and typically had aspect ratios in the ranges of 2–10:1 for the length and 1–4:1 for the width. In the core region, the particles were spherical and the same size as in the extruded pellets.

Differences in size and shape of SEBS particles in the blends derive from the interfacial tension and rheological characteristics of the components. Domains of the dispersed component are elongated in the complex flow fields of the blending and injection moulding operations. After cessation of flow, the elongated domains may relax to a spherical shape, or, if the aspect ratio is sufficiently large, they may break up by an interfacial instability mechanism. When other variables are held constant, the viscosity ratio of the two components is the decisive factor controlling the extent to which the dispersed phase is elongated in the flowing melt. Compared to the functionalized elastomers, the higher viscosity of SEBS-0MA favoured less extended domains in the melt which in turn favoured relaxation into large particles with a broad size distribution in preference to break-up into smaller particles of more uniform size. Additionally, higher interfacial tension in the non-reactive blend would have enhanced coalescence of SEBS-0MA into larger particles. The functionalized SEBS elastomers all had about the same viscosity, so viscosity alone did not account for the further decrease in particle size with increasing functionality. This was attributed to a decrease in the interfacial tension brought about by higher graft density. This would have facilitated interfacial-tension-driven break-up and reduced the tendency toward subsequent coalescence.

#### Stress-strain behaviour at ambient temperature

Tensile deformation of PET and all the blends was characterized by formation of a macro-shearband at the

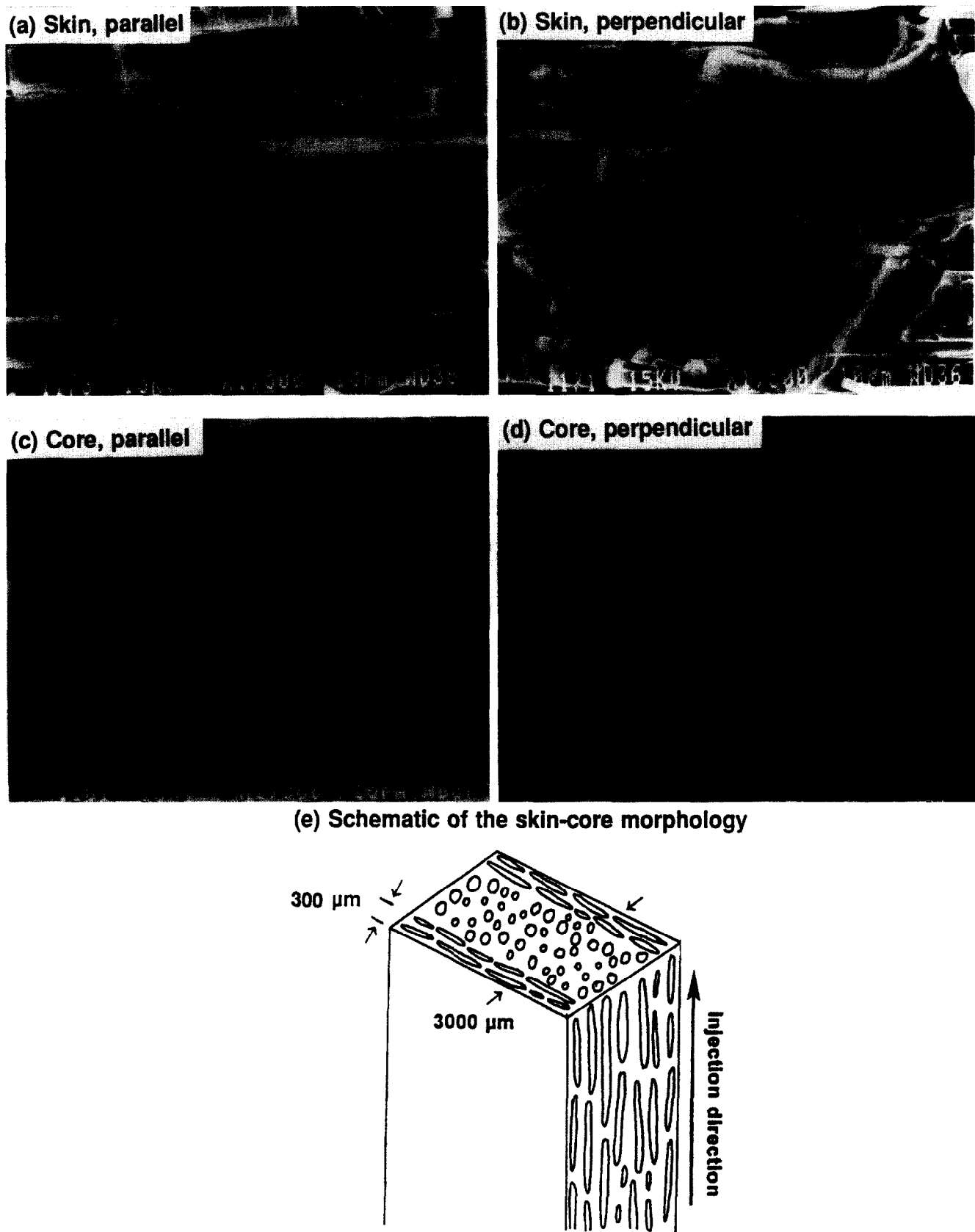


**Figure 4** Scanning electron micrographs of freeze-fractured and etched surfaces from an injection moulded tensile specimen of the 5% SEBS-0MA blend processed at 280°C/35 rpm: (a) parallel to the injection direction near the edge; (b) perpendicular to the injection direction near the edge; (c) parallel to the injection direction near the centre; (d) perpendicular to the injection direction near the centre; and (e) schematic of the skin-core morphology

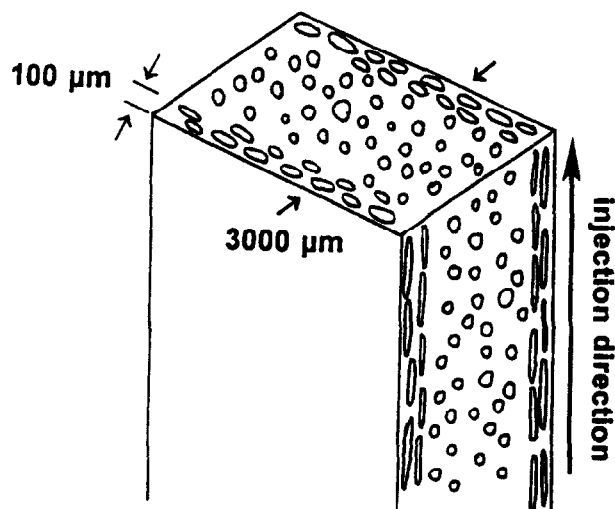
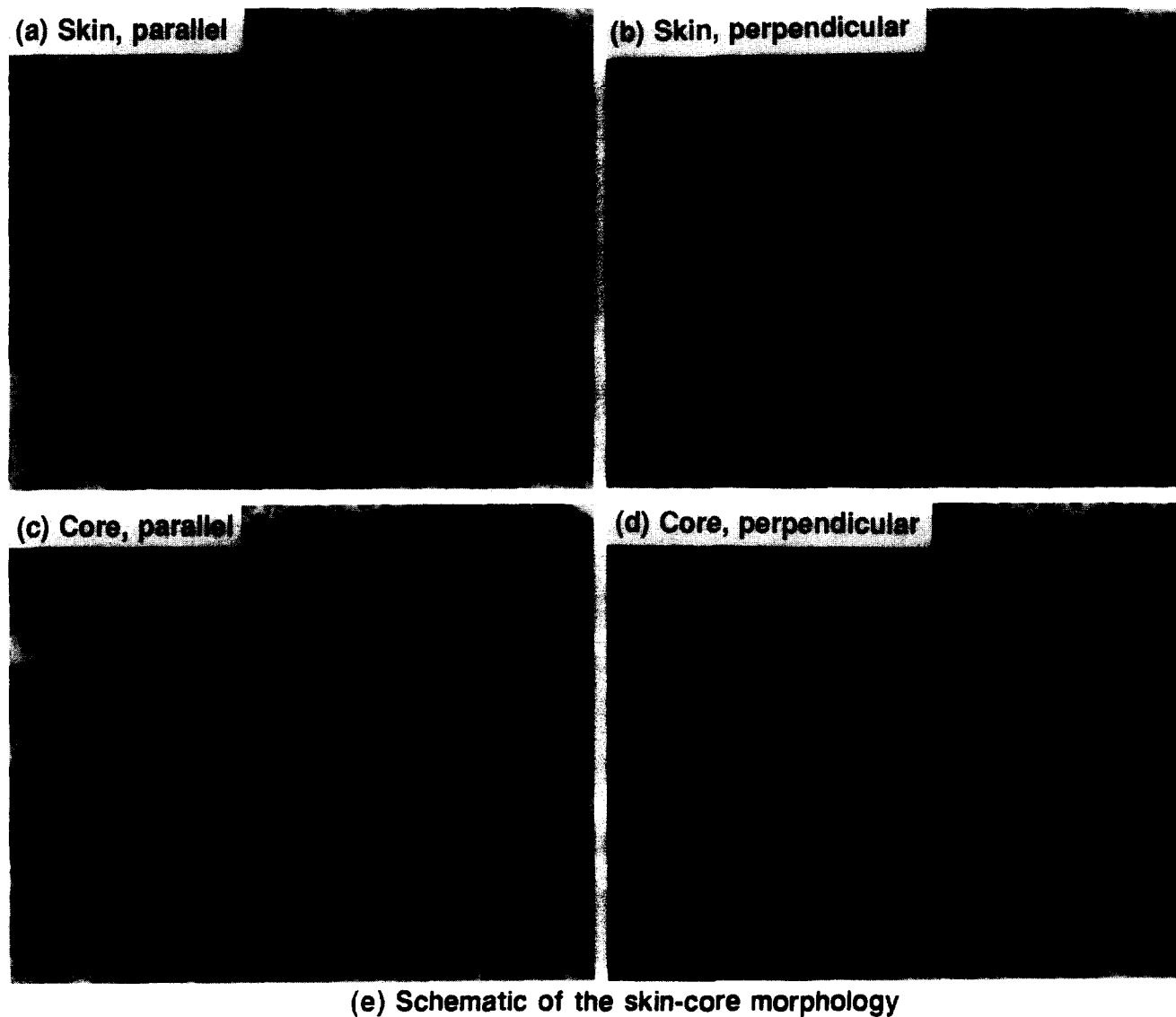


**Figure 5** Scanning electron micrographs of freeze-fractured and etched surfaces from an injection moulded tensile specimen of the 5% SEBS-2MA blend processed at 280°C/35 rpm: (a) parallel to the injection direction near the edge; (b) perpendicular to the injection direction near the edge; (c) parallel to the injection direction near the centre; (d) perpendicular to the injection direction near the centre; and (e) schematic of the skin-core morphology

yield point, followed by propagation of a neck from one side of the macro-shearband. The engineering stress dropped to about half the yield stress as the neck formed, the neck then propagated at a constant engineering stress. The yield stress decreased approximately linearly with rubber content (Table 3). The engineering draw stress and the draw ratio in the propagating neck (4.7) were essentially unaffected by blend composition.

The major effect of blending an SEBS elastomer with PET was enhanced stability of the propagating neck. Typically, PET fractured at the end of the neck after the neck had propagated only a short distance. In contrast, the neck in the blends propagated at constant stress from one side of the macro-shearband all the way to the end of the gauge section. The necked region then uniformly strain hardened with gradually increasing stress until the neck started to propagate again from the other side of the macro-shearband, accompanied by another stress drop and a second region of cold drawing. When the entire gauge section had necked, there was a region of uniform strain hardening that terminated when the

specimen fractured at one end of the neck<sup>1</sup>. In un-notched stress-strain tests carried out at a strain rate of 100% min<sup>-1</sup>, all the blends were ductile and fractured after the entire gauge section had necked.

Higher rate tests on blends with 5% SEBS elastomer resulted in lower fracture strains, however again there was no significant influence of functionality on the tensile properties (Table 3). In particular, SEBS-OMA was as effective as the functionalized SEBS elastomers in increasing the elongation at break, even though no graft copolymer was formed. The high aspect ratio of the SEBS-OMA domains in the direction of tensile deformation might have increased the ductility. The anisotropic particle shape also revealed the morphology of SEBS-OMA blends to be especially process-dependent, an otherwise undesirable feature. Morphology may not have been the sole factor, however; it has been observed that enhancement of PET properties can be achieved without good interfacial adhesion of the second phase if the degree of triaxiality is low, as in an un-notched tensile test<sup>4</sup>.

### Toughness

High speed puncture fractures of PET and the blends at 25°C were all ductile with essentially the same fracture energy (Table 4). At a lower temperature, -29°C, PET was brittle as were all the blends with 1% SEBS and 2% SEBS elastomer except for one ductile specimen with 2% SEBS-1MA. However, for blends with 5% SEBS-1MA and 5% SEBS-2MA, a majority of the five specimens fractured in a ductile manner. When ductile fractures were observed, the fracture energy increased accordingly. It would appear that blends with 5% SEBS elastomer were close to the brittle-to-ductile transition.

Blending PET with 5% of an SEBS elastomer did not significantly improve the Izod impact strength. In this regard, it should be noted that the SEBS elastomer content was considerably lower than the 20% used in previous studies where enhanced Izod impact toughness of PET was demonstrated<sup>5,6</sup>. Because the Izod test conditions were too severe to ascertain the effect of 5% SEBS elastomer on notch sensitivity of PET, specimens with the V-shaped Izod notch were tested in tension at a

Table 3 Tensile properties of blends processed at 280°C/35 rpm<sup>a</sup>

Material	<i>E</i> (GPa)	$\sigma_y$ (MPa)	$\epsilon_b$ (%)
PET	1.0 ± 0	60 ± 1	96 ± 39
	1.2 ± 0 <sup>b</sup>	63 ± 1 <sup>b</sup>	35 ± 15 <sup>b</sup>
1% SEBS-OMA	0.9 ± 0	58 ± 1	797 ± 44
2% SEBS-OMA	0.9 ± 0	57 ± 0	811 ± 30
5% SEBS-OMA	0.9 ± 0	54 ± 0	616 ± 168
	1.1 ± 0 <sup>b</sup>	55 ± 1 <sup>b</sup>	210 ± 50 <sup>b</sup>
1% SEBS-1MA	0.9 ± 0	58 ± 0	485 ± 92
2% SEBS-1MA	0.9 ± 0	56 ± 0	682 ± 124
5% SEBS-1MA	0.9 ± 0	53 ± 1	890 ± 28
	1.1 ± 0 <sup>b</sup>	57 ± 1 <sup>b</sup>	135 ± 78 <sup>b</sup>
1% SEBS-2MA	0.9 ± 0	58 ± 1	594 ± 189
2% SEBS-2MA	0.9 ± 0	55 ± 0	850 ± 50
5% SEBS-2MA	0.9 ± 0	53 ± 0	712 ± 51
	1.1 ± 0 <sup>b</sup>	58 ± 1 <sup>b</sup>	159 ± 50 <sup>b</sup>
1% SEBS-4.5MA	0.9 ± 0	58 ± 0	699 ± 89
2% SEBS-4.5MA	0.9 ± 0	56 ± 0	650 ± 194
5% SEBS-4.5MA	0.9 ± 0	52 ± 0	405 ± 150
	1.1 ± 0 <sup>b</sup>	55 ± 1 <sup>b</sup>	146 ± 35 <sup>b</sup>

<sup>a</sup> Strain rate 100% min<sup>-1</sup> unless otherwise indicated

<sup>b</sup> Tested at a strain rate of 1000% min<sup>-1</sup>

Table 4 High-speed puncture properties of PET and blends processed at 280°C/35 rpm

Material	Max. load (N)		Total energy (J)		Failure mode <sup>a</sup>
	25°C	-29°C	25°C	-29°C	
PET	1254 ± 17	673 ± 644	12.2 ± 0.2	1.6 ± 1.7	all brittle
1% SEBS-OMA	1247 ± 31	861 ± 450	14.1 ± 0.5	1.7 ± 1.1	all brittle
2% SEBS-OMA	1215 ± 16	440 ± 361	12.7 ± 0.1	0.9 ± 0.6	all brittle
5% SEBS-OMA	1202 ± 11	902 ± 232	12.4 ± 0.1	1.8 ± 0.6	all brittle
1% SEBS-1MA	1274 ± 10	181 ± 56	12.4 ± 0.6	0.3 ± 0.1	all brittle
2% SEBS-1MA	1240 ± 17	709 ± 760	12.6 ± 0.3	3.5 ± 6.3	4 brittle, 1 ductile
5% SEBS-1MA	1215 ± 12	1309 ± 810	13.7 ± 0.4	10.2 ± 8.3	2 brittle, 3 ductile
1% SEBS-2MA	1281 ± 12	366 ± 77	12.7 ± 0.3	0.7 ± 0.3	all brittle
2% SEBS-2MA	1151 ± 10	523 ± 470	12.1 ± 0.2	1.2 ± 0.9	all brittle
5% SEBS-2MA	1185 ± 18	1568 ± 486	12.4 ± 0.2	11.4 ± 5.7	1 brittle, 4 ductile
1% SEBS-4.5MA	1242 ± 30	478 ± 388	12.7 ± 0.2	1.1 ± 0.7	all brittle
2% SEBS-4.5MA	1239 ± 43	1081 ± 565	12.4 ± 0.3	3.1 ± 2.1	all brittle
5% SEBS-4.5MA	1204 ± 20	852 ± 590	11.7 ± 0.5	1.9 ± 1.2	all brittle

<sup>a</sup> Five specimens tested

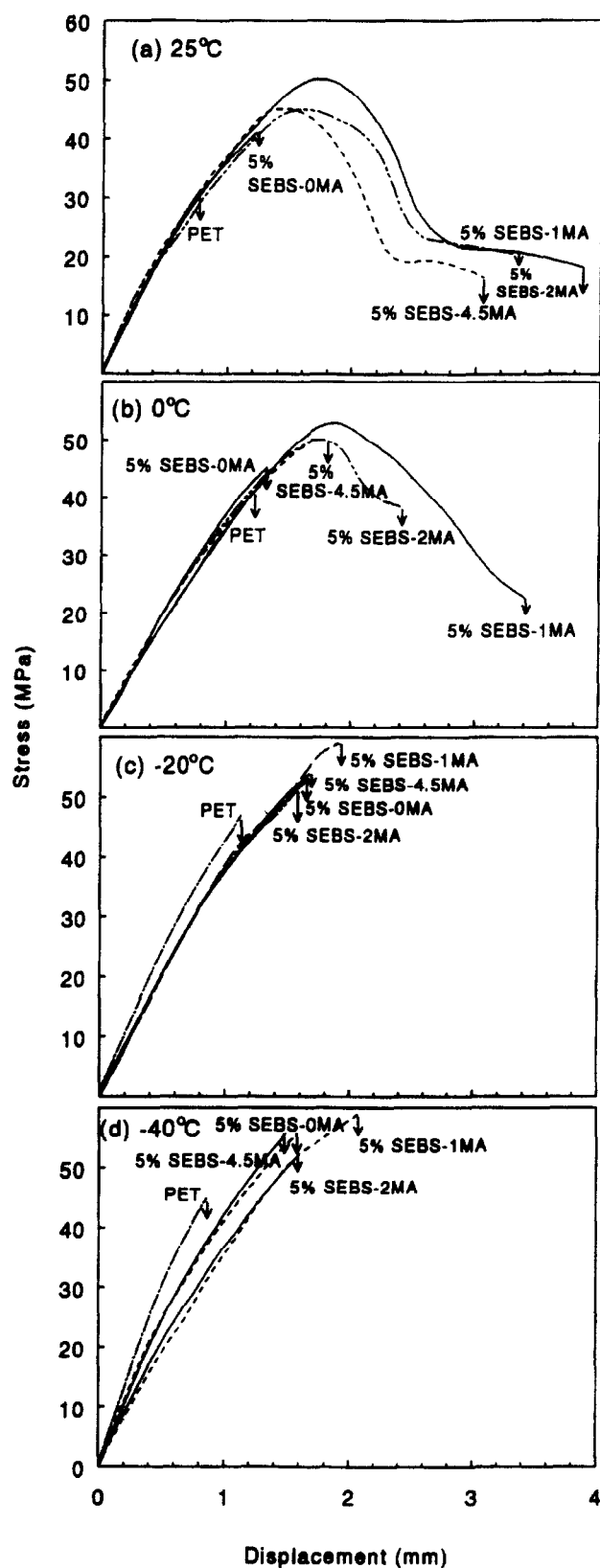


Figure 6 Stress-displacement curves of notched PET and blends with 5% SEBS elastomer tested with a crosshead speed of  $500 \text{ mm min}^{-1}$  at different temperatures: (a)  $25^\circ\text{C}$ ; (b)  $0^\circ\text{C}$ ; (c)  $-20^\circ\text{C}$ ; and (d)  $-40^\circ\text{C}$

somewhat lower rate than the effective rate of the Izod test. The test temperature was varied in order to obtain transitional behaviour that would differentiate the toughness of the blends<sup>7,8</sup>. The stress-displacement curves at three temperatures of PET and blends with

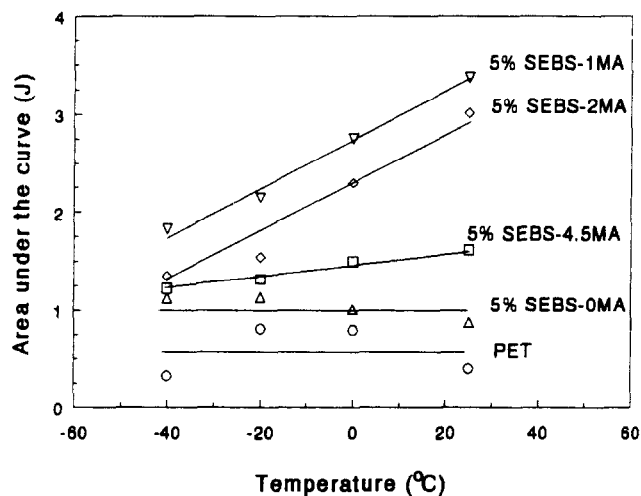


Figure 7 Area under the stress-displacement curve as a function of temperature for notched PET and blends with 5% SEBS elastomer

5% SEBS elastomer are shown in Figure 6. At  $25^\circ\text{C}$ , the blends with functionalized SEBS all yielded at the notch root in contrast to PET, which fractured in a brittle manner, and the blend with 5% SEBS-0MA, which also fractured in a brittle manner but at a higher stress than PET. Tests at  $0^\circ\text{C}$  differentiated among the blends with functionalized SEBS. The blend with 5% SEBS-4.5MA fractured in a brittle manner in contrast to the blend with 5% SEBS-1MA which remained ductile; the blend with 5% SEBS-2MA was intermediate. At  $-20^\circ\text{C}$ , all the compositions fractured in a brittle manner, but varied in the fracture stress or strain.

The blends were differentiated in terms of their reduced notch sensitivity by considering the fracture energy, taken as the area under the stress-displacement curve (Figure 7). The least effective elastomer was SEBS-0MA which increased the fracture energy of PET only slightly. In contrast, the most effective was SEBS-1MA, the functionalized SEBS with the lowest anhydride concentration. Increasing the functionality above 1% produced a decrease in the fracture energy. Both particle size and interfacial adhesion influenced these trends. The striking difference between blends with SEBS-0MA and blends with SEBS-1MA was attributed to formation of a graft copolymer by reaction between anhydride groups and PET. The graft copolymer enhanced interfacial adhesion in the solid state and reduced the domain size by reducing interfacial tension in the melt state. The subsequent trend toward decreasing toughness with increasing anhydride functionality was credited to greater cavitation resistance as the particle size decreased<sup>9</sup>.

In summary, functionalization of the SEBS elastomer is not required for enhanced ductility of PET under loading conditions that do not impose a large triaxial component. Thus, in uniaxial tension, where the only triaxial component is produced by the shape of the neck, even unfunctionalized SEBS stimulates sufficient cavitation to ensure stable neck propagation. If the conditions are more severe, as in a notched tensile test, unfunctionalized SEBS elastomer does not promote enough cavitation to reduce the notch sensitivity. This may be because the particle size is too large and/or the adhesion is too poor. Under these conditions, effective relief of the triaxiality requires good adhesion between matrix and



elastomer. This is achieved with *in situ* formation of a graft copolymer by reaction of anhydride groups grafted on the SEBS with hydroxyl end groups of the PET. In addition to providing good adhesion, the graft copolymer strongly reduces particle size and also reduces process sensitivity of the morphology, i.e. the tendency for particle shape and orientation to reflect the flow field. Although functionalization of the SEBS is more important than the actual anhydride concentration, there does appear to be an optimum. In this system increasing the anhydride concentration on the SEBS, which means increasing the number of potential graft sites, slightly decreases the toughness. This is attributed to the effect of graft copolymer structure on particle size.

#### ACKNOWLEDGEMENT

The generous financial support of the Shell Chemical Company is gratefully acknowledged.

#### REFERENCES

1. Tanrattanakul, V., Perkins, W. G., Massey, F. L., Moet, A., Hiltner, A. and Baer, E., *Polymer*, 1997, **38**, 2191.
2. Han, C. D., *Multiphase Flow in Polymer Processing*. Academic Press, New York, 1981, Chap. 4.
3. Chuang, H.-K. and Han, C. D., in *Polymer Blends and Composites in Multiphase Systems*, ed. C. D. Han, *Advances in Chemistry* 206. ACS, Washington, 1984, p. 181.
4. Wilfong, D. L., Hiltner, A. and Baer, E., *J. Mater. Sci.*, 1986, **21**, 2014.
5. Gelles, R., Modic, K. M. and Kirkpatrick, J., *SPE ANTEC Tech. Papers*, 1988, **34**, 513.
6. Penco, M., Pastorino, M. A., Occhiello, E., Garbassi, F., Braglia, R. and Giannotta, G., *J. Appl. Polym. Sci.*, 1995, **57**, 329.
7. Tse, A., Laakso, R., Baer, E. and Hiltner, A., *J. Appl. Polym. Sci.*, 1991, **42**, 1205.
8. Dijkstra, K., ter Laak, J. and Gaymans, R. J., *Polymer*, 1994, **35**, 315.
9. Dompas, D., Groeninckx, G., Isogawa, M., Hasegawa, T. and Kadokura, M., *Polymer*, 1994, **35**, 4750.